Excimer Lasers and Optics

Ting Shan Luk
Chair/Editor

Proceedings of SPIE—The International Society for Optical Engineering

Volume 710

Excimer Lasers and Optics

Ting Shan Luk
Chair/Editor

Sponsored by
SPIE—The International Society for Optical Engineering

Cooperating Organizations
Center for Applied Optics/University of Alabama in Huntsville
Center for Electro-Optics/University of Dayton
Georgia Institute of Technology
Institute of Optics/University of Rochester
Optical Sciences Center/University of Arizona
Tufts University/Electro-Optics Technology Center

18–19 September 1986
Cambridge, Massachusetts

Published by
SPIE—The International Society for Optical Engineering
P.O. Box 10, Bellingham, Washington 98227-0010 USA
Telephone 206/676-3290 (Pacific Time) • Telex 46-7053

The papers appearing in this book comprise the proceedings of the meeting mentioned on the cover and title page. They reflect the authors' opinions and are published as presented and without change, in the interests of timely dissemination. Their inclusion in this publication does not necessarily constitute endorsement by the editors or by SPIE.

Please use the following format to cite material from this book:
Author(s), "Title of Paper," *Excimer Lasers and Optics*, Ting Shan Luk, Editor, Proc. SPIE 710, page numbers (1987).

Library of Congress Catalog Card No. 86-62867
ISBN 0-89252-745-5

Printed in the United States of America.

EXCIMER LASERS AND OPTICS

Volume 710

INTRODUCTION

The excimer laser has become one of the most important gas lasers in the ultraviolet wavelength region in recent years. Many aspects of its importance were presented at this conference. The conference was divided into three sessions: Session 1, Research and Development I; Session 2, Material Processing; and Session 3, Research and Development II.

The content of these sessions includes both reviews and new developments in areas concerning: fundamental research in excimer lasers (710-18, -19, and -21); excimer laser development (710-01, -02, -03, -05, -06, -13, -16, -20, -22, and -23); and applications of excimer lasers in nonlinear phenomena (710-14, -15, -16, and -17), material processing (710-07, -08, -09, -10, -11, and -12), and spectroscopic studies (710-16, -17, -18, and -19).

In the scope of excimer laser development, commercial lasers have made impressive progress in generating high average power in the 100-W range, high repetition rates in hundreds of pulses per second, and good reliability (710-01). Lasers with high pulse energy on the scale of a kilojoule per pulse (710-05 and -20) and high peak power with tens of gigawatts using picosecond technology (710-06, -15, and -16) are the new records. In addition, development efforts are focusing on specific qualities like compactness (710-02), long pulse duration (710-22), and large aperture discharges (710-23)—all challenging new technological grounds. Finally, the sol-gel technology shows a promising outlook for achieving higher damage threshold optics for excimer lasers.

In the community of excimer laser users, manufacturers, and researchers, resourcefulness in imagining new applications has proven to be beneficial. Specific processes like marking and modification of finished products have provided new insights to applications (710-11). Excimer lasers have contributed significantly to the understanding of the laser melting (710-07) and etching processes (710-10). They have the advantages of allowing speckle-free exposure to the workpiece and having a small penetration depth. These properties were shown to be very important in solar cell processing (710-12) and laser lithography (710-08). The large photon energy property of excimer lasers allows a chemical reaction to be initiated by a single photon process. This shows promise for wide use in the laser photochemical vapor deposition process in the semiconductor industry (710-09). Furthermore, efficient excimer lasers have become the workhorse of laser fusion programs (710-05) and x-ray laser research (710-16 and -17). Medical applications using excimer lasers, though not included in this conference, are addressed in other conferences. The editor regrets that the topic of self-phase conjugation using excimer lasers is not covered.

Fundamental research efforts continue to accumulate spectroscopy data on excimers (710-18 and -19), thus providing new insights and guidelines in the development and extension of excimer laser sources (710-21).

Ting Shan Luk
University of Illinois at Chicago

EXCIMER LASERS AND OPTICS

Volume 710

Contents

EXCIMER LASERS AND OPTICS

Volume 710

Session 1

Research and Development I

Chair
Ting Shan Luk
University of Illinois at Chicago

High Average Power Commercial Excimer Lasers

Jack Andrellos, Mary Essary and Herbert Pummer
Lambda Physik, U.S., 289 Great Road, Acton, MA 01720 U.S.A.

High power excimer lasers which can deliver average powers of 100 W or more have been commercially available since 1983 when Lambda Physik introduced its model EMG 203 MSC. This progress was the result of a new proprietary switching technique (Magnetic Switch Control or MSC) which allowed unprecedented control of the energy flow through the high voltage discharge circuitry. In conjunction with a carefully designed gas flow and the judicious choice of components, this technique has meanwhile enabled the design of a large variety of reliable excimer systems including injection locked systems, lasers which deliver 120 W average power and lasers which can operate at up to 1000 Hz pulse repetition rate.

At present the excimer laser market is driven by a variety of technical requests from the industrial and scientific communities including narrow bandwidths for scientific and photolithographic applications, high repetition rates for averaging, homogeneity of energy distribution and others. However at the core of most discussions two key issues tend to appear: a) reliability with respect to catastrophic component failure and b) maintenance cycles with the associated question of component lifetime.

It is interesting to note that the tremendous progress which excimer lasers have made with respect to these very issues has at the same time made it difficult to address these questions. Lifetime testing a variety of components with lifetimes in the 10^9 shots range in a system which operates at a pulse repetition rate of 200 Hz for example, takes approximately six months. Naturally such tests have to be performed on a sufficiently large number of systems to obtain any statistically significant data and it is easy to show that the costs involved exceed the resources of most excimer laser manufacturers.

Caught between this fact and the justified questions from customers regarding reliability and lifetime data, some manufacturers have resorted to substantial extrapolations or have based their information on a very small number of samples, a situation in which it may not always be easy to maintain objectivity. Obviously it would be desirable to have both, that is, a thorough lifetime testing by the manufacturer together with feedback from a broad customer base. Interestingly such a sample does indeed exist.

At present by far the largest installed excimer laser base is the MSC type lasers. Since their introduction in 1983 approximately 500 systems have been installed worldwide, providing a sizeable sample over a considerable time span. Approximately one third of these lasers can operate at pulse repetition rates of 200 Hz or more. The work load on lasers varies from light use in low duty cycle scientific applications to heavy use in scientific and industrial applications. Customers who invest in the higher priced high repetition rate excimer laser models usually do so because of their experimental requirements. Such a high repetition rate laser accumulates nearly 10^6 shots per hour and it is therefore clear that the installed base described above contains a significant number of units which have operated between 10^8-10^9 shots.

When doing a reliability analysis on excimer laser components it is imperative to recognize that the statistics which governs failure due to normal wear and tear are completely different from the statistics which describes catastrophic failure. While the former displays the predictable and well defined lifetime of a component (e.g., an electrode) in the form of a narrow distribution, the occurence of catastrophic failure due to its unpredictability - is described by a very wide statistical distribution. This implies immediately that valuable information about electrode lifetimes, for example, can be gained from the controlled testing of a small but representative sample. Such work has been performed in Lambda Physik's 24-hour testing facility since May 1985 and has resulted in the systematic improvement of component lifetimes for optics, preionizers, electrodes, etc.

On the other hand, it is equally obvious that catastrophic failure cannot be judged from small samples. Fortuitously this disadvantage is offset by the fact that - once a large sample is available - solid information about component reliability can be obtained, even though the sample represents a widely varying spectrum of uses.

The list of excimer laser components which traditionally have been critical with respect to catastrophic failure is short. It contains the thyratron and the high voltage capacitors.

An analysis of the available data - as obtained from the sample of 500 lasers over three years - shows that the performance of Lambda Physik excimer lasers which are equipped with the new technology has indeed become quite impressive.

Component	Failures
High voltage capacitors	1
Thyratrons	2
MSC switch	none

Here the MSC switch, although clearly being a long lifetime passive element, is included because it represents a comparatively novel element in excimer lasers.

These data reflect a high voltage capacitor and thyratron failure rate amounting to only a fraction of one percent. The fact that all three cases occured at rather low shot numbers points towards failure caused by a faulty component rather than by the operational parameters. In such a large sample the failure data indicate directly that the sample - although having been exposed to extensive use - is not anywhere near the maximum of the failure curve. This in turn allows one to give lower limit lifetime figures for the corresponding component. Combining this finding with internal life testing data we arrive at the following evaluation:

COMPONENT LIFETIME

•OPTICS	$>5 \times 10^8$
•ELECTRODES	1×10^8 (ArF) 5×10^8 others
•PREIONIZER	1×10^8 (ArF) 5×10^8 others
•THYRATRON	$>10^9$
•CAPACITORS	$>10^9$
•HV POWER SUPPLY	$>10^9$
•MAGNETIC SWITCH	5×10^9

Based on these lifetimes, one arrives at the following recommended maintenance schedule:

ROUTINE MAINTENANCE

•OPTICS CLEANING	10^8
•HALOGEN FILTER	5×10^8 XeCl
•OPTICS EXCHANGE	5×10^8
•ELECTRODE/PREIONIZER REPLACEMENT	5×10^8

A major overhaul of the laser would include exchange of the thyratron and the high voltage capacitors at 10^9 shots or more. It is interesting to note that 10^9 shots correspond to approximately 3 years of operation if the laser is running at 200 Hz repetition rate with a 25% duty cycle for 8 hours per workday. In this scenario the total cost for parts would only amount to approximately $5,000 per year.

Beyond progress in discharge technology, component reliability and gas lifetimes, the flexibility and performance of excimer laser systems has seen considerable progress. An example is the EMG 150/160T MSC which offers high power capabilities for materials processing, as well as linewidth and frequency control which satisfy requirements of UV Raman spectroscopy and photolithography. In addition the system can simultaneously operate on two different excimer wavelengths for a large variety of other applications.

Basically the EMG 160 MSC consists of two laser heads whose discharges are switched through a common Magnetic Switch in order to simplify the discharge circuitry and to guarantee temporal synchronization. The EMG 150 MSC can operate at pulse repetition rates of up to 80 Hz while the EMG 160 MSC reaches 250 Hz. The two laser heads operate from independent gas manifolds which allows the fine adjustment of gas fill parameters for optimum system performance as well as two color operation.

Dependent on the needs of the user, the two heads can be operated and connected to each other in a variety of optical configurations which are easily interchangeable.

In applications where high average power at low divergence is desired, one of the laser heads (the oscillator) is equipped with unstable resonator optics, producing a beam of 0.2 mrad divergence. This beam is then passed through the second laser head (the amplifier) in a single pass. This arrangement results in average powers of 40 W ArF, 100 W KrF and 45 W XeCl. When stable resonator optics are used in the oscillator average powers exceeding 120 W in KrF can be reached. In this configuration the EMG 160 MSC is one of the most powerful excimer lasers currently available.

Applications can have stringent requirements with respect to narrow bandwidth and frequency stability, for example in UV Raman spectroscopy and photolithography. Because both applications place a premium on high repetition rates it is mandatory for the system not to relax in these specifications towards higher repetition rates.

In the narrow bandwidth mode the oscillator of the EMG 160 MSC is equipped with a grating-tunable resonator. The narrow bandwidth output from this resonator is injected into the unstable resonator structure of the amplifier where it locks the available energy to the narrow bandwidth with an efficiency which exceeds 95%. This arrangement delivers a bandwidth of 0.3 cm^{-1} and average powers of 16 W ArF, 60 W KrF and 33 W XeCl. An additional intracavity etalon in the oscillator can further reduce the bandwidth to below 0.1 cm^{-1}. The tuning range is approximately 1 nm.

The frequency stability of this system in the 0.3 cm^{-1} version was tested with an etalon-reticon combination of 0.05 cm^{-1} resolution. Both the shot to shot frequency jitter as well as the long term frequency drift over a continuous two hour run were smaller than this resolution. Significantly these results were obtained at the highest repetition rates and are valid for operation at 193 nm, 248 nm and 308 nm.

This excellent stability has been made possible by a new design which positions all critical optical components on a joint honeycomb platform vibrationally isolated from the laser head. A well designed gas flow allows operation of up to 250 Hz. The pointing stability of the whole assembly, like the frequency stability, is excellent.

In the two color mode each laser head can be fitted with either stable or unstable resonator optics and can independently be operated at any excimer wavelength. Again the pulses from the two lasers are temporally well synchronized. Pulse energies and average powers from the oscillator head are 115 mJ/15 W ArF, 260 mJ/60 W KrF, 100 mJ/20 W XeCl while the amplifier head delivers 130 mJ/20 W ArF, 290 mJ/65 W KrF and 140 mJ/35 W XeCl.

Such systems represent the most accurate, versatile and powerful excimer lasers available.

Inductively Stabilized Excimer Lasers

Robert C. Sze*
Los Alamos National Laboratory
Los Alamos, New Mexico 87545

Abstract

We review the work at Los Alamos regarding long pulse excimer laser operation using the technique of inductive stabilization of avalanche discharges. This technique, depending on the rate of energy deposition, has allowed laser pulse lengths of greater than 120ns and total lasing times greater than 200ns. Small lasers employing this technique are particularly useful in the control of large amplifiers to obtain narrow linewidth, near diffraction limited operation as well as in the amplification of mode-locked pulse trains to further enhance the brightness of the laser system. The performance of small lasers with short cavity length used for narrow-band frequency tuning, active modelocking and the advantages associated with high repetition rate operation will be discussed. The scaling to longer gain lengths and to high average power systems will also be discussed. Finally, a brief discussion of the potential uses of small long pulse devices in the areas of high brightness sources, medical and semiconductor applications will be given.

Introduction:

It is well known that conventional rare-gas halide excimer lasers excited in avalanche discharges have relatively short stable discharge times. The application of soft x-rays to introduce extremely uniform preionization into the medium shows promise in the possibility of extending the stability time of the discharge. Compact commercial devices utilizing this technique needs the development of very compact x-ray preionizing sources. The development of corona bar cathodes by Helionetics and of the wire ion plasma (WIP) guns (first developed at Hughes and being used at Livermore, Northrop and the Institut de Mecanique des Fluides in France) for the x-ray preionization source tells us that large energy devices of relatively long pulse durations should be in the market place in the near future.

This talk deals with a much simpler technique for achieving long excimer laser pulses. This is the technique of inductive stabilization of excimer avalanche discharges which allows for simplified pulse power circuits with much slower energy deposition. The only complication rests in a segmented electrode structure with each segment ballasted by a stabilizing inductor. The possibility that this was a viable technique to achieve long pulse stable avalanche discharges in excimer laser gas mixtures is due to the work of the Oxford University laser group under Colin Webb[1,2,3]. They showed that long pulse XeCl lasers was possible when the discharge was ballasted by resistive carbon rods. Subsequently, Sze and co-workers at Los Alamos have shown that viable high repetition rate, long pulse excimer lasers are achieved using inductive ballasting[4,5].

General Characteristics:

A series of three generation of devices have been built at Los Alamos. The initial lasers are built with no or very low flow capabilities in insulated vessels. The active discharge length is of some 28cm with active electrode lengths of some 20cm. We have constructed discharge devices of small active discharge volumes and by varying the active discharge volume have deposited energy successfully from 30 joules per liter atmosphere to as high as 300 joules per liter atmosphere at 3 atmospheres in time scales of total deposition times of approximately 200ns. The preionization is of the corona type which required small amounts of peaking capacitance with resultant modulation of the energy deposition. Recent computer modeling of the pulse power show that it is possible to elimate this modulation and recent experimental work in our laboratory using simplified circuits have realized unmodulated lasing times greater than 70ns. We have observed a saturation of the energy deposition which result in lasing times somewhat shorter than the electrical energy deposition time. At deposition levels of 30 joules per liter atmosphere or less, lasing times equivalent to the energy deposition times are achieved. Lasing efficiencies at these short discharge lengths are in the region of 1% for XeCl and KrF and less for XeF.

A striking characteristic of the inductively stabilized laser is the order of magnitude gains in pulse repetition rate per unit gas flow. Thus, it appears possible to construct very compact high repetition rate devices giving good average power (in the 5 watts to 30 watts level) using this technique. Our second laser device is locally known as the V-8 laser because two laser heads were incorporated in a vessel with a small 2 inch tangential blower. The laser heads are connected in parallel with respect to the pulse power and in series with

respect to the flow. This small device can operate at kilohertz pulse repetition rates. Average powers in XeCl is at the 4 watts level with a much reduced energy deposition per pulse into a small 4mmX4mm discharge area. Such long pulse laser devices are especially promising in laser angioplasty and in direct write semiconductor applications.

Our third laser device is a modular laser system called the Stablex laser where modular lengths scaling of the laser is possible. In a four module system we have achieved in a 1cmX1cm area laser energies greater than 175mj per pulse in XeCl. Efficiencies near 1.5% are measured. There has been some arcing in this laser. We believe when these minor problems are solved efficiencies in the 3% region will be observed. Further, we intend to double the discharge gap separation to 2cm which should double the energy per pulse. Thus, we look toward operation in the 400-500 watts average power range at pulse repetition frequencies in the 1 kilohertz region.

We feel that the inductive stabilization technique has allowed for important gains in pulse length and pulse repetition rate over more conventional laser systems. Lasers using this technique and operating at kilohertz pulse repetition rates and at energies of 1 joule per pulse should be possible. Scaling to even higher energies may be problematic due to the size of the electrode area controllable by one inductor. Thus, very large electrodes will mean an extremely complicated electrode structure.

Applications:

The most widespread application at Los Alamos is the use of these long pulse laser devices as oscillators to control high energy short pulse amplifiers. In the pursuit of this application we have shown that as narrow linewidth tunable sources a gain of 40 per given dispersion due to the increased pulse length is observed. The reason for this gain have been presented6 and is related to the increased number of round trips of the tuned oscillator. We have achieved active mode-locking of these long pulsed excimer lasers giving pulse widths shorter than 200ps with pulse to pulse separations less than 2.8ns. These pulses have been amplified using 1cmX1cm area of an Lambda-Physik EMG201 laser. With one microjoule per pulse input a gain of 1500 is measured resulting in single pass energies for the pulse train of greater than 40 millijoules. The goal here is to obtain an intermediate brightness source of high average energy in the pulse train to generate a continuously tunable vacuum uv source in the region between 80 to 120nm for neutral particle beam sensing applications.

Small long pulse lasers of very compact size are especially attractive in laser angioplasty applications. Energy transmission through optical fibers should increase proportional to the ratio of the pulse lengths. Indeed, recent study by a group from a medical company using our laser obtained a 100 times increase in transmission through a 100 micron fiber over short pulse lasers with a pulse length increase of only some ten times. They attrbute the added order of magnitude increase to the improved beam uniformity of the stabilized laser system. Finally, we feel that the compact long pulse laser system should be especially useful in semiconductor manufacturing in the area of direct writing as the increased pulse length improves the duty factor of the laser, thus, increasing the writing speed.

*Presently on leave at the Institut de Mecanique des Fluides, Universitat Aix-Marseille II, 13009 Marseille, France

References:

1. K. Kugii, A.J. Kearsley, A.J. Andrews, K.H. Erry, and C.E. Webb (1981) IEEE J. Quantum Electron. QE-17, 1315

2. D.C. Hogan, A.J. Kearsley, and C.E. Webb (1980), J. Phys. D 13,L225

3. D.C. Hogan, R. Burzzese, A.J. Kearsley, and C.E. Webb (1981), J. Phys. D 14, L157

4. R.C. Sze, J. Appl. Phys.,54, 1224 (1983)

5. R.C. Sze, Inst. Phys. Conf. Ser. No.72, 227, paper presented at the 5th GLC Symp., Oxford 1984; Adam Hilger Ltd. 1985

6. R.C. Sze, N.A. Kurnit, D.E. Watkins and I.J. Bigio,"Narrow band tuning with small long-pulse excimer lasers", (Invited Paper) presented at the Int'l Conf. on Lasers '85, Las Vegas, Nev. (Dec. 1985); to be published in Proceedings of the conference.

Characteristics of E-Beam Pumped KrF Laser System

K.Ueda, H.Nishioka, and H.Takuma

Institute for Laser Science, Univ. of Electro-Communications
1-5-1 Chofugaoka, Chofu-shi, Tokyo 108 Japan

Abstract

The charcteristics of strongly saturated amplifier with a 100ns electron beam excitation are studied to determine the small signal gain, non-saturable absorption, and saturation intensity from 6% Kr to 95% Kr in Ar diluent. The pumping rates are maintained constant by adjusting the total pressure of gas mixtures to conpensate the different stopping power of Ar and Kr. Non-saturable absorption coefficients are measured at a full saturated amplifier between the zero gain intensity to 80MW/cm^2. The small signal gain of 12.9%/cm and non-saturable absorption coefficient of 1.32%/cm are obtained for 95% Kr mixture. The saturation intensity, 2.2MW/cm^2 for 6% Kr and 2.9MW/cm^2 for 95% Kr mixture, derived from the zero gain intensity is in good agreement with the prediction of our computer model. Highest intrinsic efficiency of 12.2% is measured at high Kr concentration where the extraction power density of 6.8MW/cm^2 is obtained by the probe laser beam between 5-6MW/cm^2. The formation efficiency for a wide range of Kr concentrations agrees with the theoretical prediction excellently as a function of Kr concentration. The details of the important parameters, gain , absorption, saturation intensity, maximum output, intrinsic efficiency, extraction efficiency, and formation efficiency will be discussed in this paper.

1. Introduction

All the recent studies of the target inplosion experiments have made it sure that short wavelength lasers are most promising for the inertial confinement fusion driver (ICF driver).[1,2] The volume and the aperture of power amplifier for practical reactor driver are estimated too large to apply a ultra violet crystal to the large aperture window.[3] The wavelength of KrF laser is the shortest among the high power excimer lasers above the transmission limit of fused silica without serious optical damages. The high efficiency of the KrF laser is of great advantage to the other short wavelength lasers. In a previous paper, we reported the high efficiency performance of our KrF laser oscillator that the output of 80J was obtained with the highest intrinsic efficiency above 10% in a low Kr concentration gas mixture.

In a last few years, many papers have been published about the high Kr concentration operation of KrF laser.[4,5] In a Kr rich KrF laser, the pressure of the laser cell at a high pumping rate is around one atmosphere where the mechanical stress in a large window is reduced. Besides the low pressure operation, most of the simulation studies predicted that the efficiency of a KrF laser would rise considerablly at high Kr concentrations due to the efficient formation of KrF*. However the results of experimental studies were not always in agreement with the prediction of kinetic simulation. The accuracy of the basic parameters such as gain, absorption and saturation intensity was not so good to discuss about the detail of the kinetics up to the present. In this paper, we will measure the absorption measurements at strongly saturated amplifier, and discuss about the formation and intrinsic efficiency related to the Kr concentration of an electron beam pumped KrF laser.

2.Theory

2-1 Theoretical Analysis of Amplifier

Supposing the effective life time of a KrF excimer is shorter than a pulse duration of input, the behavior is analysed with a steady state approximation. Mangano[6] modified the wellknown Rigrod analysis by introducing a distributed, non-saturable absorption. Rice[7] extended the formulation to include the effect of F_2 absorption in the unpumped regions and loss by the cell windows. In the steady state analysis, the density of KrF* (N) in the upper laser level is given by a partially differential equation

$$\frac{\partial N}{\partial t} = R_p - \left(\frac{1}{\tau} + \frac{\sigma I}{h\nu}\right) \quad \text{(steady state)} \quad (1)$$

where R_p is the pump rate into the upper laser level, τ is the life time of the level including the spontaneous emission and collisional quenching, σ is the cross-section of spontaneous emission, I is the photon flux density (W/cm^2), and $h\nu$ is the energy of the single photon. The variation of the photon flux as a function of position along the axis is given by

$$\frac{\partial I}{\partial z} = (g - a_n)I \quad (2)$$

where g_0 is the small signal gain (cm^{-1}), ,and a_0 is the non-saturable absorption. Gain saturation is described using a saturation intensity Is.

$$g = \frac{g_0 - a_0}{1 + I/Is}$$

where the small signal gain $g_0 = \sigma R_p \tau$, and the saturation intensity $Is = h\nu/\sigma\tau$. The re-

lationship between the input and output after passing the active length of L is derived by integration (2) from z=0 to L.

$$\ln\left(\frac{Io}{Ii}\right) = (g_0 - a_n)L + \gamma \ln\left(\frac{Io - Is(\gamma-1)}{Ii - Is(\gamma-1)}\right) \quad (4)$$

where γ is defined as gain to non-saturable loss ratio given by g_0/a_n. The definitions of g_0 and Is yield the formation rate from the total energy entering into the upper laser level.

$$E = h\nu R_p L = g_0 Is L \quad (5)$$

The extraction efficiency with which a probe beam extracts the available power from the amplifier is given by

$$\eta_{ext} = \frac{Io - Ii}{h\nu R_p L} = \frac{Io - Ii}{g_0 Is L} \quad (6)$$

The product of a formation efficiency and a extraction efficiency yields the intrinsic efficiency as follows.

$$\eta_{int} = \eta_{form}\eta_{ext} = \frac{Io - Ii}{Pump} \quad (7)$$

2-2 Saturation of Non-Saturable Absorption

In the theoretical analysis described above, we assumed that the saturable absorption had the same saturation intensity as that of gain saturation, and the non-saturable absorption did not saturate for extremely high intensity input. The possibility of the saturation of non-saturable absorption at extremely high intensity field have to be checked before the strongly saturated amplification, because most of the absorption species of KrF laser are short lived ionized or excited species of low density. If the saturation intensity of the non-saturable absorption is defind as $Is_{ab} = \beta Is$, the output intnsity is given in a following relation,

$$\ln\left(\frac{Io}{Ii}\right) = (g_0 - a_n)L + \frac{\gamma(1-\beta)^2}{(\gamma-\beta)^2}\ln\left(\frac{Io + \beta\frac{(\gamma-1)}{\gamma-\beta}Is}{Ii + \beta\frac{(\gamma-1)}{\gamma-\beta}Is}\right) - \frac{\gamma-1}{\gamma-\beta}\frac{Io-Ii}{Is} \quad (8)$$

When the absorption is intrinsically non-saturable, this equation is analytically equal to (4) by inserting $\beta=0$. The characteristics of the absorption saturation is shown in Fig.1(a). The absorption maxima are observed in a full saturation region due to the absorption saturation. The input intensity at the absorption maximum is plotted in Fig.1(b) as a function of saturation intensity of absorption. Even if the saturation intensity is above 300MW/cm^2, the input intensity at the absorption maximum is predicted below 60MW/cm^2. Therefore the absorption saturation at very high intensity is detectable if the maximum intensity of 100MW/cm^2 is available for the gain - measurement.

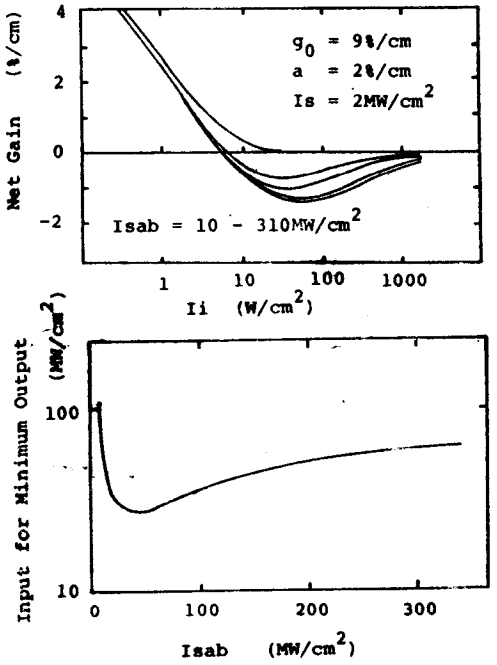

Fig.1 Saturation of absorption is detectable from the gain minimum below 100MW/cm^2.

2-3 Condition of Constant Gain

Although the solution of the Rigrod analysis is strict over a wide range of intensity, it is very difficult to determine the gain, absorption, and saturation intensity simultaneously. Some papers reported the absorption measurements by using a slightly off resonant probe beam.[8,9] However the spectral shape of the KrF laser absorbers are not wellknown, so that the accuracy of the absorption coefficient is not good - enough. In this paper, we will try to measure the absorption coefficient directly in the same scheme of the gain measurement.

When the input intensity is low enough, the gain coefficient is independent on the input intensity. So the accuracy of the small signal net gain $(g_0-a_0)-a_n$ is good. Similar condition is attained at an extremely high intensity field. Assuming that the input intensity is two order of magnitude higher than the saturation intensity, the saturated gain is much smaller than the non-saturable absorption. In this case, the probe beam is absorbed in the amplifier with a constant absorption factor. Another constant gain is zero. The effective gain is always zero along the axis for the zero gain intensity that gives the maximum output intensity of a oscillator. The zero gain input intensity I_0 is related to the saturation intensity Is in a following relation,

$$I_0 = Is\ (\gamma - 1) \quad (9)$$

When the non-saturable absorption is measured in a full saturation amplifier, the small signal gain is derived easily by

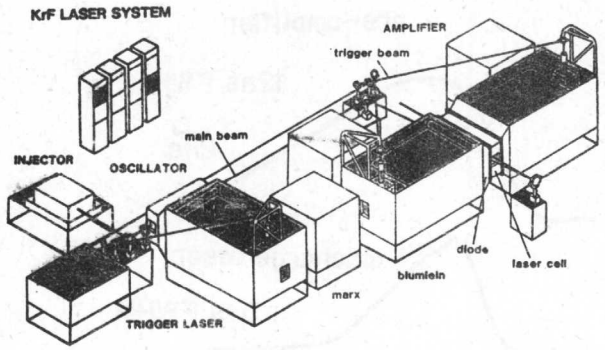

Fig.2 E-beam pumped KrF Laser System

adding the small signal net gain and the non-saturable absorption. After the determination of gain to loss ratio g_0/a_n, the zero gain intensity I_0 yields the saturation intensity by using (9). This is a very simple way to determine the direct determination of laser parameter by a gain measurement of constant amplification factor. In addition to the simplicity, the accuracy of the measured absorption will become higher because the experimental condition is absorption dominant region.

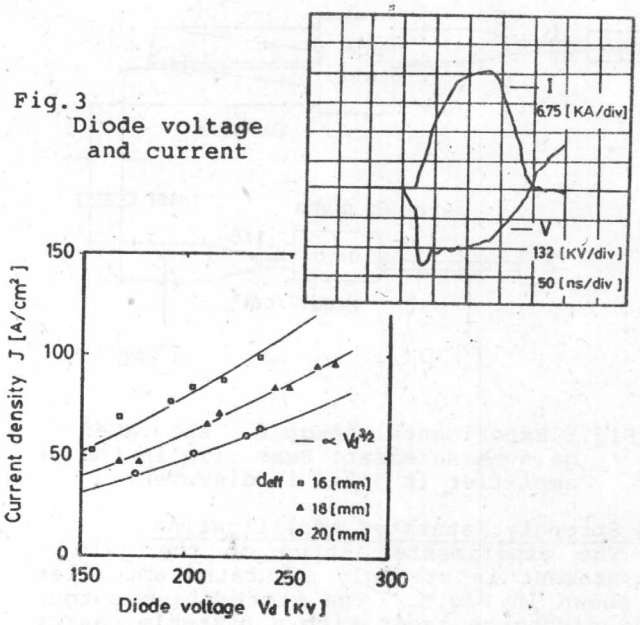

Fig.3 Diode voltage and current

Fig 4 Comparison with the C-L law. The solid lines are theoretical curve.

3. Experiments

3-1 Experimental Apparatus

The electron beam pumped KrF laser system used in this study involves two discharge lasers and two electron beam excited amplifier. All the electron beam generators are synchronized by the KrF laser triggered switches of the 10 ohms water dielectric parallel plate Blumlein. The diode operates at a maximum voltage of 300kV with a current density of 110A/cm^2. The pulse duration of electron beam current is 120ns. The amplifier cell is 1m long with an excitation region of 40cm. The length of excitation region is designed to eliminate the energy depletion due to the amplified spontaneous emission. Fused silica windows are angled at 5 degree from the axis to reduce the feedback from the windows. All the windows and lenses are uncoated to prevent the optical damage up to 200MW/cm^2.

3-2 Diode Characteristics

The waveforms of diode voltage and diode current are shown in Fig.3. Taking into consideration of the space charge effect, the diode characteristics are completely in agreement with the Child-Langmuir law at every instant as shown in Fig.4 where the solid lines give the theoretical curves including the plasma expansion effect. The plasma drift velocity is constant at 6×10^6cm/s after the plasma turn-on time. For the anode and pressure foils our original carbon coated Kapton films are used to reduce the transmission loss. The variation of the electron beam output is less than 5%, and the life time of CCK films is more than 1000 shots.

3-3 Pumping Rate

Total deposition energy is measured by a fast response pressure transducer, Kyowa model PG20KU . The deposition profile of the electron beam excitation is calculated by a Monte-Carlo code. To check the reliability of the calculated profile, the small signal gain distribution is measured for the opposed beam pumped main amplifier. A large aperture, uniform beam is injected into the amplifier cell by using a large magnification beam expander. The amplified beam by a small signal gain factor is detected by a CCD camera after the wavelength conversion from UV to VIS on the fluorescent plate. The amplified image is transfered to the image processor, and the analyzed gain distribution is compared with the calculated deposition profile. The calculated deposition profile is in good agreement with the measured gain distribution between 1 to 2.5atm. As for the stopping power of gas mixtures, we refere the table of Bearger and Seltzer.[10] The local pumping rate at the distance of 1.5cm apart from the pressure foil of beam A is measured 1.1MW/cm^3 . For the higher pumping density, the A-K spacing of the other side (e-beam B) is slightly closed so that the deposition rate is estimated 1.4MW/cm^3. The pumping rate is maintained at the constant rate by adjusting the total pressure for the gas mixtures of different Kr concentration. For example, a mixture of 736 Torr Kr, and 39Torr Ar has the same stopping power as a mixture of 83 Torr Kr, and 1307 Torr. The F_2 concentration of 4 Torr is optimized to the high Kr concentration. This is slightly lower than the optimum F_2 density of Ar rich KrF laser.

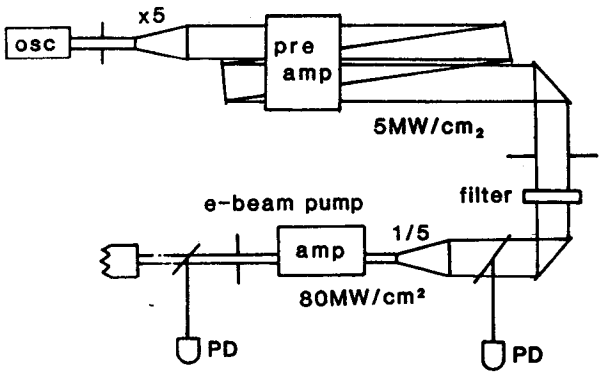

Fig.5 Experimental setup for saturated gain measurement. Beam size in the amplifier is 3.2mm in diameter.

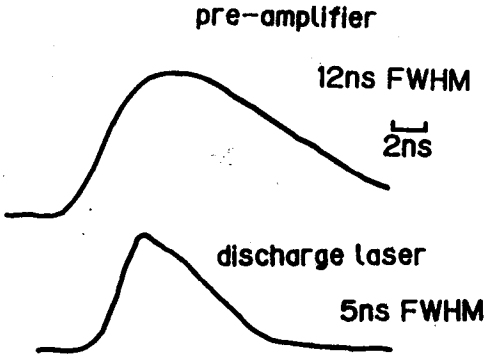

Fig.6 Waveform of the probe beam

3-4 Strongly Saturated Amplification

The experimental setup of the gain - measurement in strongly saturated amplifier is shown in Fig.5. The short pulse output of a discharge laser with a unstable cavity is apmlified by an electron beam pumped pre-amplifier after the beam expansion of factor 5. Partial reflective mirrors and UV filters (IMP filters) are inserted in a low intensity region below 4MW/cm^2. The probe beam is collimated by a telescope with a reduction of diameter from 16mm to 3.2mm. The tripple pass ASE and the scattered components of the input aperture and optics are separated by the output iris of 5mm in diameter. The output energy is - measured by a Scientech 38-0103 volume absorbing calorimeter. The surface reflections of the thin fused silica are detected by photo diodes, Hamamatu R1193U. The detector signals are recorded in transient digitizers (Iwasaki model 8123), and data are transfered to the computer memory.

3-5 Optical Damage by Probe Beam

Maximum input intensity available in the gain measurement is limited by the damage threshold of a fused silica window or lens. The damage threshold of dielectric coating is much lower than that of rear surface of the fused silica window. The pulse duration has to be controled as short as possible to achieve the higher input intensity without optical damage. The short pulse discharge laser of 5ns pulse duration is prepared for the oscillator of the probe beam. Futhermore the optical configuration of pre-amplifier is designed to shorten the pulse duration by using a gain saturation due to the beam overlap between second and tripple pass beams. A typical waveforms of probe beam before and behind the pre-amplifier. The extention of the pulse duration is due to the saturation amplification in pre-amplifier. Below 200MW/cm^2, the sample of a fused silica is free from any optical damage. Multiple shots of 400MW/cm^2 pulse produces a small damage on the surface, and the single shot damage is observed at 600-MW/cm^2. The maximum output intensity of the pre-amplifier is approximately between 4 to 5MW/cm^2 due to the gain saturation. Supposing the magnification factor of output telescope is 5, maximum input intensity from 80 to 90MW/cm^2 is available for gain measurements with the reflective losses of the optics. According to the calculated saturation intensity of 6% Kr mixture of 2.3MW/cm^2, the gain decreases by a factor of 40 at 90MW/cm^2 where the absorption is dominant in the amplifier.

4. Results and Discussions

4-1 General Features of Gain Measurement

At first, the characteristics of the Ar rich KrF amplifier, 6% Kr in Ar diluent, are studied for a wide range of input intensity. The variation of amplifier gain as a function of input intensity from 375W/cm^2 to 80MW/cm^2 is shown in Fig.7. All the data are measured at the peak of the deposition rate of e-beam excitation. Small signal gain is measured by the attenuated probe beam without excitation in pre-amplifier. The small signal net gain g_0-a_0-a_n

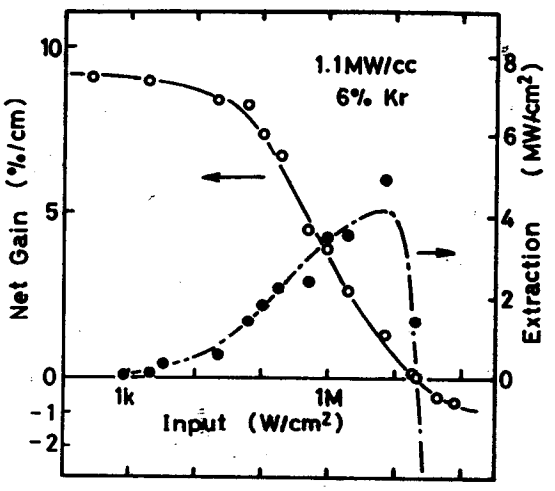

Fig.7 Gain and extraction as a function of input intensity.

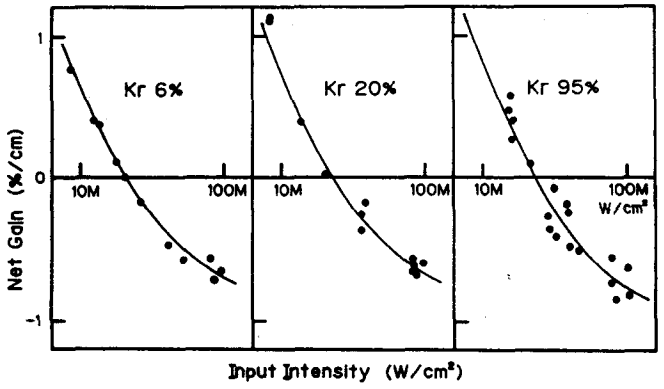

Fig.8 Strongly saturated Gain

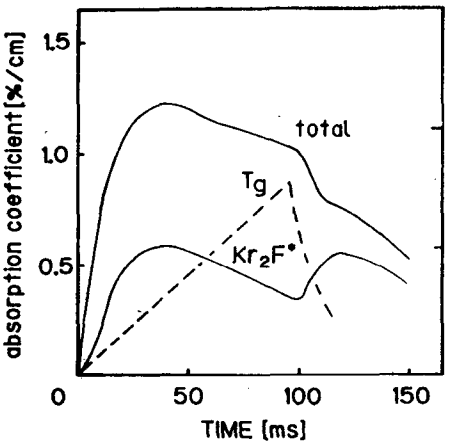

Fig.9 Time variation of absorption during the e-beam pulse. Absorption drop of Kr_2F^* is due to the gas temperature.

is determined for low intensity input below 3kW/cm^2. As the input intensity increases through the triple pass pre-amplifier, the amplifier gain decreases monotonously until the the saturated gain is smaller than the non-saturable absorption. However the residual gain is not negligible at 80MW/cm^2 although the gain is strongly saturated. In order to determine the non-saurable absorption with a error smaller than 10%, the absorption coefficient is determined by the curve fitting in the strongly saturated region. Zero gain input intensity is observed clearly in the gain curve beteween 20 and 30MW/cm^2 in Fig.7. The extracted power from the amplifier is also measured directly. The second curve in Fig.7 shows the estimated extraction power I_e-I_i calculated using the gain fitting curve. As predicted in the theoretical analysis, the extraction has a maximum value at the input intensity about $Is(\gamma-1)$. If we can measure the detail of the peak extraction condition, the intrinsic efficiency of the strongly saturated amplifier is directly measured. It seems very easy to measure the non-saturable absorption in Fig.7. These results encourages us to study the details of saturated amplifier intensively.

4-2 Non-Saturable Absorption

Qantitative studies of the e-beam pumped KrF laser are carried out under the pumping rate of 1.1MW/cm^3 and 1.4MW/cm^3 for 6% Kr, 20% Kr, and 95% Kr gas mixture. In the following, the detailed discussion will be focused to the 1.1MW/cm^3 pumping case. The results of gain measurement at extremely high input intensity are plotted in Fig.8 with the fitting curves. The experimental error seems to affect the absorption of the order of 0.1%/cm^2. According to the extraporations of the approximation curves, non-saturable absorption coefficient given in Fig.8 for the 6%, 20%, and 95% Kr mixtures are 0.95, 0.95, and 1.1%/cm^2, respectively. Below 80MW/cm^2, the net gain increases monotonously as the input intensity increases. According to the theoretical prediction, the saturation of the absorbers is small in this experimant.

Major non-saturable absorbers in the KrF laser are considered as F_2, F^-, Kr_2^+, Kr**-(5p), Ar_2^+, Ar**(4p). In a simple idea, it seems probable that the reduction in Ar_2^+ population for high Kr concentration mixtures enables a lower non-saturable absorption because the photo-absorption cross-section at 248nm of Ar_2^+ is a factor of 5 larger than Kr_2^+. On the other hand, the absorption of Kr** is a factor of 20 larger than Ar**. It is very difficult to estimate the net absorption of gas mixtures involving many compensation processes as a function of Kr concentration in a qualitative discussion. In a qantitative analysis using a kinetic code, the absorption shows a tendency to increase as a function of Kr concentration. The calculation results suggest that the change of the absorption is moderate because the reaction kinetics of the gas mixtures are stabilized through the complex compensation processes. The predictions of our kinetic code for the non-saturable absorption are 0.72%/cm for 6% Kr mixture, and 1.1%/cm for 95% Kr mixture, respectively. From the comparison with the code predictions, the absorption for high Kr concentration is reasonable.

Some fractions of large absorption at high Kr concentration are due to the temperature dependence of the absorption cross-sections of Ar_2^+ and Kr_2^+ because the sensitivity of Kr_2^+ absorption for the gas temperature is a factor of 4 higher than Ar_2^+.

4-3 Small Signal Gain

Small signal gain measurements are carried out using the attenuated discharge laser output from 300 to 400 W/cm^2. The small signal net gain $g_0-a_0-a_n$ is constant at 9 %/cm for every gas mixture. The small signal net gain g_0-a_0 is almost constant at 1.1MW/cm^3 for every Kr concentration mixtures. According to the kinetic code calculations, the saturable absorption due to

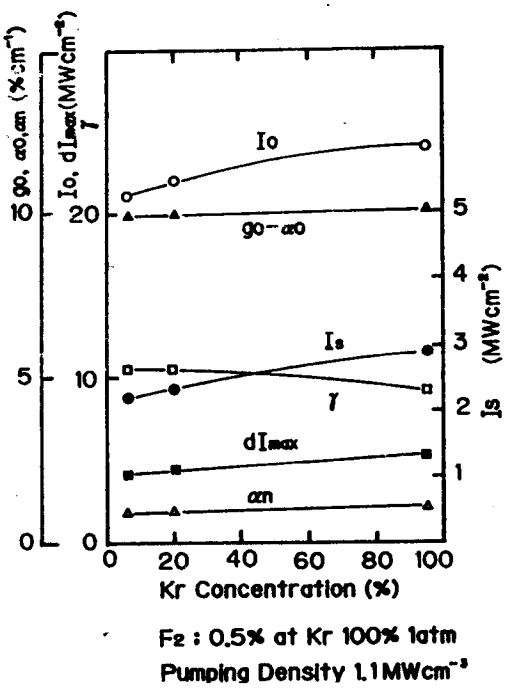

Fig.10 KrF laser parameters as a function of Kr concentration under constant pumping of 1.1MW/cc, where g_0-a_0 is small signal net gain, a_n is non-saturable absorption, Is is gain saturation intensity, I_0 is zero gain input, γ is gain to loss ratio, and dImax is maximum extraction, respectively.

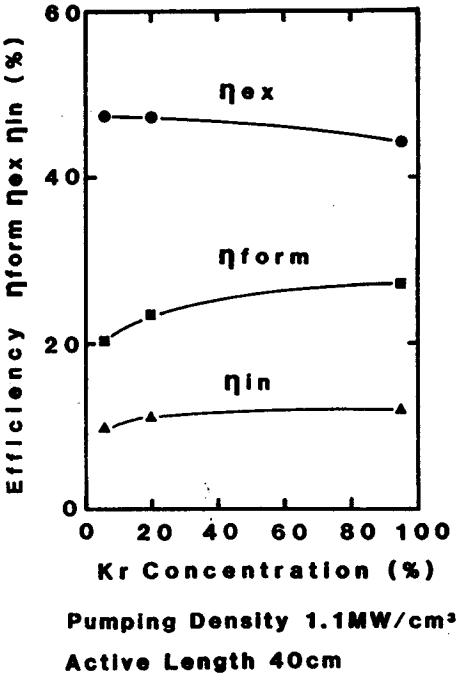

Fig.11 KrF laser efficiency

Kr_2F^* decreases 50% during the e-beam pumping as shown in Fig.9, although the non-saturable absorption is constant. The Kr_2F^* formation reaction through the 3 body collision reduces the population of Kr_2F^* as a function of $T_g^{-1/3}$. In this study, the gas temperature at the probe beam input rises 80K from the initial temperature for 6% Kr in Ar diluent. The absorption of Kr_2F^* is estimated 48% of the initial value at the front of electron beam. In the case of 95% Kr mixture, the gas heating is more effective due to the high stopping power, and the gas temperature is estimated 144K higher. Assuming the saturable absorption of 0.4%/cm for 6% Kr and 0.2%/cm for 95%/cm, the small signal gain g_0 is nearly constant over the Kr concentration.

4-4 Saturation Intensity

As shown in Fig.8, zero gain intensities are measured directly in the high intensity gain measurement. By solving the equation (2) at the steady state condition, the relation between the zero gain intensity and saturation intensity is given by

$$I_0 = Is(\gamma - 1) = Is\left(\frac{g_0-a_0}{a_n} - 1\right) \qquad (10)$$

Measured gain to lass ratio $(g_0-a_0)/a_n$ is 10.5 for Ar rich gas and 9.2 for Kr rich mixture. From the zero gain intensity, the saturation intensities for 6% Kr, 20% Kr, and 95% Kr are determined 2.2, 2.35, and 2.9MW/cm^2, respectively. High saturation intensity in high Kr concentration corresponds to the fast quenching in Kr rich mixtures compared with the Ar diluent gas mixture. The predictions of the saturation intensity using our kinetic code is in good agreement with the measured values within 5%.

4-5 Formation and Extraction Efficiency

From the theoretical consideration above, the formation efficiency of upper laser level is given by the produnt of a small signal gain and a saturation intensity. The measured formation efficiency for the 95% Kr mixture is listed in Table 1. The formation efficiency of upper laser level of 95% Kr is a factor of 1.35 higher than that of low Kr concentration.

Empirically, it is known that 24.3 eV is required to form an electron-ion pair from Kr. In the case of 95% Kr mixture, the major part of KrF* is formed through the following ionic recombination channels,

$$Kr^+ + F^- + M \rightarrow KrF^* + M$$
$$Kr_2^+ + F^- \rightarrow KrF^* + Kr$$

The residual KrF* can form from Kr* by the way of harpoon reaction as follows,

$$Kr^* + F_2 \rightarrow KrF^* + F$$

Assuming the additional yield of 0.35 Kr* metastable to the ionic reactions, the theoretical formation efficiency for Kr/F_2 mixture is 28%. The measured formation efficiency for 95 % Kr is in excellent agreement with the theoretical value.